ELSEVIER

Ceramics International 27 (2001) 801–807

CERAMICS INTERNATIONAL

www.elsevier.com/locate/ceramint

Hydration-resistant lime refractories from Egyptian limestone and ilmenite raw materials

A.G.M. Othman[a,*], M.A. Abou El-Maaty[b], M.A. Serry[a]

[a]*Refractories, Ceramics and Building Materials Department and Geological & Geophysical Department, National Research Center, 12622- Dokki, Cairo, Egypt*

[b]*Geological & Geophysical Department, National Research Center, 12622- Dokki, Cairo, Egypt*

Received 2 October 2000; received in revised form 29 November 2000; accepted 12 January 2001

Abstract

Four refractory lime batches were processed from the pure limestone economically available at Beni Khaled, El Menia, Egypt up to firing at 1550°C using a two-stage firing process. The ferri-ilmenite ore existing at Abu Ghalaga, Eastern Desert was added as a dopant material in amounts of 0.5, 1.0, 2.0, 3.0%. Densification parameters and hydration resistance of the fired grains were investigated. The most dense hydration resistant grains were selected to assess their refractory quality by determining load-bearing capacity and thermal shock resistance. These results were interpreted in the light of phase composition and microstructure of the fired grains. It is concluded that dense and hydration resistant lime grains can be processed by doping the pure limestone powder with 2.0–3.0 wt.% of ferri-ilmenite before firing up to 1550°C. Such level of ilmenite content has contributed in the densification of lime particles in the solid state and also by limited amount of the developed liquid phase. Hence, direct-bonded lime network is formed with partial interruption by a platey calcium–alumino–ferrite–titanate phase, which crystallized on cooling from the liquid phase at the grain boundaries of the lime–lime network. This improves the bulk density of fired grains to about 3.2–3.3 g/cm^3 and its rate of hydration to 4.15–3.80 g/h without significant deterioration of its load-bearing capacity and thermal shock resistance.
© 2001 Elsevier Science Ltd and Techna S.r.l. All rights reserved.

Keywords: Limestone; Ilmenite; Hydration resistant; Lime refractories; Dense grains; Thermal shock; Thermomechanical

1. Introduction

Due to the shortage of natural magnesite deposits suitable for manufacturing basic refractories in Egypt, some trials were done to precipitate pure magnesium hydroxide (brucite) from the available dolomite rock as well as sea-water and its brines [1–3]. Also some available basic raw materials were assessed for the production of CaO–MgO refractories; namely, MgO- dolomite, dolomite and lime refractories. These include dolomitic magnesite, dolomite and limestone [4–6].

Different grades of limestone are widely distributed over a vast territory in Egypt. High-grade limestones suitable for the iron and steel industry and other purposes are quarried at Beni Khaled locality, East Samalout, El-Menia Governerate (Fig. 1). An area of about 50 km^2 is covered by snow-white, massive and nummulitic limestone belonging to Samalout Formation of Middle Eocene age. The reserves of limestone, which is mainly composed of 98.0% calcite ($CaCO_3$), are estimated to more than 5000 million tons [7,8]. Such grade of limestone is adequate for processing dense and hydration-resistant lime refractories [6,9].

Lime (CaO) is one of the most favorable basic refractory oxides because of its high fusion point (2600°C) as well as lower vapor pressure and higher stability than MgO in the presence of carbon at high temperatures which improves its resistance to attack by siliceous slags [10–12]. For these advantages lime can be used successfully to substitute MgO-bearing refractories for lining basic oxygen steel converters as well as cement, lime kilns and secondary steelmaking ladles [13–16].

Unfortunately, hydration in contact with water or water vapor creates difficulties in its manufacture and usage. After 1960, intensive research work has been done in order to increase hydration resistance of lime. This improvement includes enhanced sintering of lime by addition of some oxides and by controlling the firing rate as well as coating the fired lime grains by impregnating

* Corresponding author. Fax: +20-0233-70931.
E-mail address: agmothman@yalla.com (A.G.M. Othman).

0272-8842/01/$20.00 © 2001 Elsevier Science Ltd and Techna S.r.l. All rights reserved.
PII: S0272-8842(01)00033-5

with tar or pitch [17–21]. The addition of some oxides, such as Fe_2O_3, TiO_2, Al_2O_3, ZrO_2 [17,19,20,22] as well as La_2O_3 and CeO_2 [23,24] has enhanced sintering of lime, yielding dense grains with improved hydration resistance. This is mainly attributed to enhancement of bulk diffusion in the solid state and also by developing limited amount of liquid phase, which can wet lime grain boundaries. The latter effect leads, however, to limited degradation of refractoriness, hot strength and slag-attack resistance of the dense lime grains [17–24].

Egyptian ilmenite ore was previously used as a dopant material with amounts of 1–4% in order to accelerate the densification rate of dolomite and MgO- dolomite materials [25,26]. This led to process low- flux, hydration-resistant and refractory grains suitable for the production of shaped and unshaped refractories. An Egyptian ilmenite deposit is located at Wadi Abu Ghalaga, 100 km south Mersa Alam and 20 km west of Abu Ghuson Port in the Eastern Desert (Fig. 1). The mineralization occurs as bands or lenses of massive ore intercalated with gabbro layers; or it forms dissemination (scattered grains) in the enclosing gabbro. The main ilmenite ore exists as upper brownish (oxidized) zone and lower black (fresh) zone [8,27]. The ore reserves were estimated to be about 40 million tons according to the mapping and borehole drilling data given by the Geological Survey of Egypt [28].

The aim of the present work is to process dense and hydration- resistant lime grains with acceptable refractory quality by using Egyptian limestone and ilmenite raw materials.

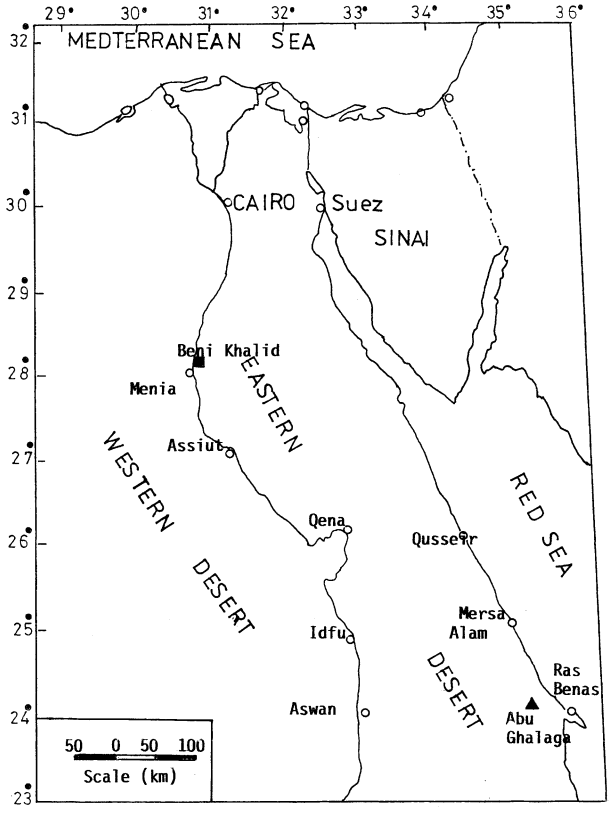

Fig. 1. Location map of the studied raw materials.

2. Materials and experimental methods

2.1. Materials

A technological sample of 100 kg was made from both Beni Khaled limestone and Abou Ghalaga ilmenite deposits representing all of their occurrences. Fig. 2(a and b) exhibits microstructure of limestone and ilmenite samples as revealed by polarizing microscopy. Fig. 2(a) shows recrystallization of sparry calcite in micritic, fossileferrous and massive limestone of Beni Khaled. The XRD pattern of this sample as shown in Fig. 3(a) confirms the presence of calcite ($CaCO_3$) as a major mineral.

Microscopic examination of a polished surface of the ilmenite ore revealed that ilmenite mineral ($FeTiO_3$) is the most abundant opaque mineral, beside some hematite (Fe_2O_3) and silicate minerals. The ilmenite occurs either as granular aggregates or as separate grains surrounded

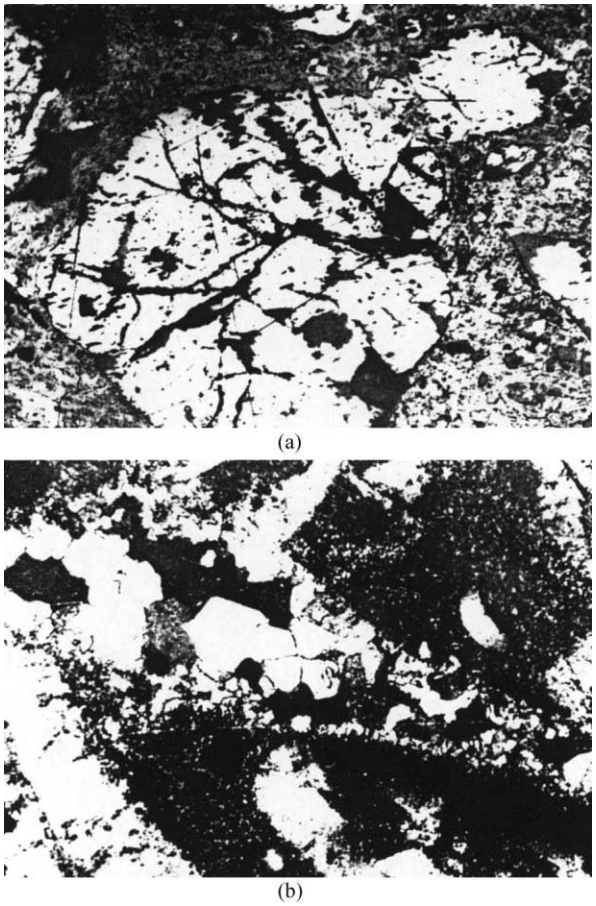

Fig. 2. (a) Photomicrograph showing fractured ilmenite crystal surrounded and corroded by silicate minerals (R.L.,×75). (b) Photomicrograph showing recrystallization of sparry calcite in micritic fossiliferous massive limestone (C.N., ×75).

and corroded by silicate minerals as shown in Fig. 2(b). By using high-magnification, hematite–ilmenite exsolutions and intergrowths form the main texture of the ore. This ore is classified as ferri-ilmenite [27]. The XRD pattern of Fig. 3(b) reveals the co-existence of ilmenite and hematite as main minerals of the ilmenite ore.

2.2. Experimental methods

Four powdered ilmenite: limestone batches, with different weight ratios of 0.5: 99.5, 1.0: 99.0, 2.0: 98.0 and 3.0: 97.0 referred to as $CI_{0.5}$, CI_1, CI_2 and CI_3, respectively, were mixed, semi-dry pressed and fired using the two- stage firing technique [16,29], i.e. calcined at 1000°C, reground, repressed and refired for 2 h at 1550°C.

Phase composition of the fired batches was qualitatively determined by the XRD technique and was also quantitatively calculated [29]. Densification parameters of the fired samples as bulk density (BD) and apparent porosity (AP) were measured by the liquid displacement method [16]. Also, cold crushing strength (CCS) was determined according to the Egyptian Standard No. 2057- 91. Microstructure was investigated by using a scanning electron microscopy (SEM, Philips XL 30) attached with an EDS unit using an accelerating voltage 30 kV, magnification of 500X and a resolution of w. (3.5 nm). The refractory quality of selected samples was assessed by measuring their refractoriness under load (RUL) according to the ISO standard No: 1893, 1st edition (1989) as well as the thermal shock resistance (TSR) by using the air- quenching method [16]. The hydration resistance was also determined by means of amount of $Ca(OH)_2$ formed after soaking lime grains in water vapor under atmospheric pressure up to 16.0 h [6].

3. Results and discussion

Table 1 and Fig. 3 show chemical and mineralogical composition of the starting materials. It is indicated that

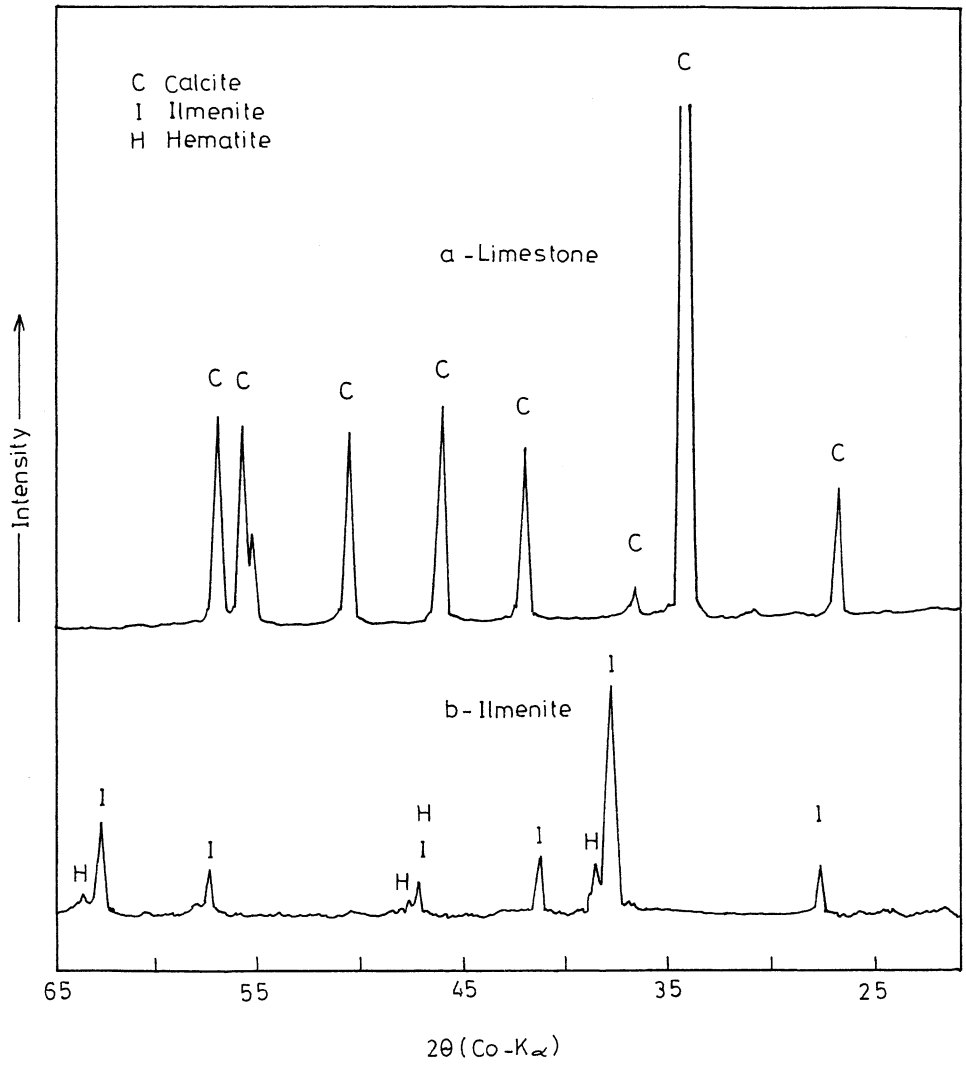

Fig. 3. XRD pattern of starting materials.

the limestone has a high degree of purity; it contains $\geqslant$98.0 wt.% CaO on calcined basis, beside small amounts of impurity oxides; namely, SiO_2 (0.53%), Al_2O_3 (1.17%) and Fe_2O_3 (0.07%). On the other hand, the main constituents of ilmenite are Fe_2O_3 (52.48%), TiO_2 (37.00%), SiO_2 6.00%), MgO (2.70%) and Al_2O_3 (1.30%) beside minor amount of CaO (0.40%). The XRD patterns of Fig. 3 confirm the purity of limestone. Limestone is mainly composed of calcite ($CaCO_3$), while the main lines detected for the ilmenite raw material are belonging to ilmenite mineral ($FeTiO_3$), beside few lines of hematite (Fe_2O_3).

Solid phase composition of the processed limestone-ilmenite batches fired up to 1550°C as calculated according to White [29] is illustrated in Table 2. These data indicate that all of the fired samples are composed of small amounts of Ca-compounds; namely, C_3S, C_4AF, C_3A, C_3T_2 phases, beside the main CaO phase due to its much high CaO/SiO_2 molar ratio. The content of Ca- compounds are increased at the expense of lime as the amount of ilmenite increased and reaches its maximum in CI_3 (2.6% C_3S, 5.0% C_4AF and 2.3%C_3T_2). The amount of C_3A is simultaneously decreased in the same direction according to the formation of increased amount of C_4AF phase. Meanwhile, the amount of free CaO decreases as the amount of impurities increases from $CI_{0.5}$ to CI_3. The amount of residual free lime is ranging between 93.0% in $CI_{0.5}$ and 89.5% in CI_3.

Densification parameters namely; bulk density (BD) and apparent porosity (AP) of the lime–ilmenite batches fired for 2 h at 1550°C are shown in Fig. 4. As the amount of ilmenite increases from 0.5 up to 2%, BD gradually increases from 3.02 to 3.23 g/cm^3. Further addition of ilmenite up to 3% leads to slight increase in BD to 3.26 g/cm^3. In contrast, AP decreases from 1.18 to 0.20% in the same order. This is attributed to the development of liquid phase during firing in increasing order from $CI_{0.5}$ to CI_3 as the amounts of C_3S, C_4AF and C_3T_2 phases are increased as illustrated in Table 2. Furthermore, there is no effective change observed on increasing the amount of ilmenite from 2 to 3%. This indicates that sintering of lime is improved by its doping with 2–3% ilmenite and firing for 2 h at 1550°C. This is accompanied with parallel improvement of the hydration resistance of the dense grains. Fig. 5 exhibits an appreciable decrease in hydration rate of CI_2 and CI_3 as compared with $CI_{0.5}$ and CI_1. The rate of formation of $Ca(OH)_2$ decreases from 2.50 g/h in $CI_{0.5}$ to 1.70 g/h in CI_3 after soaking in water vapor at 70°C under atmospheric pressure for 8 h. After 16 h soaking, the hydration rate is reduced to 3.80 g/h in CI_3, as compared with $CI_{0.5}$ (4.70 g/h). This is mainly attributed to coating of lime particles with the Ca- aluminoferrite and titanate phases, expected to precipitate from the formed liquid phase on cooling such lime grains. Accordingly, CI_2 and CI_3 are selected for phase composition, microstructure and technological properties investigations.

Fig. 6 exhibits XRD patterns of the dense CI_2 and CI_3 lime grains. Lime (CaO) is the main phase detected with relatively higher XRD intensity in CI_2 than CI_3 according to the higher lime consumption with increasing ilmenite addition. Also, few weak lines of CTAF solid solution, C_3S and $Ca(OH)_2$ are shown. The formation of small amount of $Ca(OH)_2$ reflects the high resistance of these grains to hydration in air during their preparation for XRD. These results confirm the calculated phase composition of both grains as illustrated in Table 2.

Microstructure and microchemistry of the dense CI_2 and CI_3 lime grains as revealed by SEM and EDAX are shown in Fig. 7 and Table 3, respectively. SEM photomicrographs of both CI_2 and CI_3 reflect the dense nature of the produced lime grains. Both show direct bonded lime particles with well defined rounded boundaries and almost homogenous grain growth. The diameter of lime particles are between 20 and 60 μm. These major particles are almost composed of pure CaO as shown from point analyses No. 2 in both CI_2 and CI_3. The direct bonded lime network is clearly interrupted by some calcium alumino–ferrite titanate plates

Table 1
Chemical analysis of the starting materials (wt.%)

Oxide	Limestone	Ilmenite
SiO_2	0.53	6.00
Al_2O_3	1.17	1.30
Fe_2O_3	0.07	52.48
TiO_2	–	37.00
CaO	98.09	0.40
MgO	–	2.70

Table 2
Chemical and phase composition of the fired batches

Batch	Batch composition (%)		Chemical composition (%)						C/S m. ratio	Solid phase composition (%)				
	Lime	Ilmenite	SiO_2	Al_2O_3	Fe_2O_3	TiO_2	CaO	MgO		C_3S	C_4AF	C_3A	C_3T_2	CaO
CI 0.5	99.5	0.5	0.56	1.17	0.33	0.19	97.60	0.01	188	2.1	1.0	2.5	0.4	94.9
CI 1	99.0	1.0	0.58	1.17	0.59	0.37	97.11	0.03	179	2.2	1.81	2.1	0.8	93.0
CI 2	98.0	2.0	0.64	1.17	1.12	0.74	96.14	0.05	160	2.4	3.4	1.2	1.6	91.2
CI 3	97.0	3.0	0.69	1.17	1.64	1.11	95.16	0.08	148	2.6	5.0	0.3	2.3	89.5

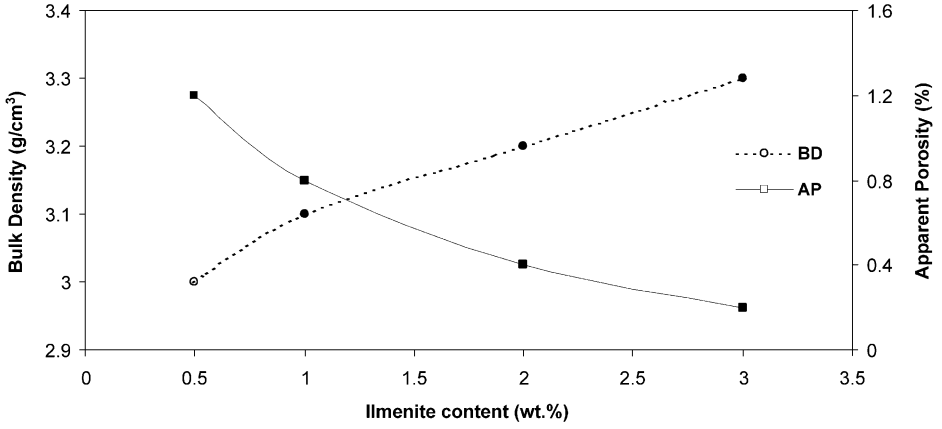

Fig. 4. Densification parameters of lime–ilmenite samples fired for 2 h at 1550°C as a function of ilmenite content.

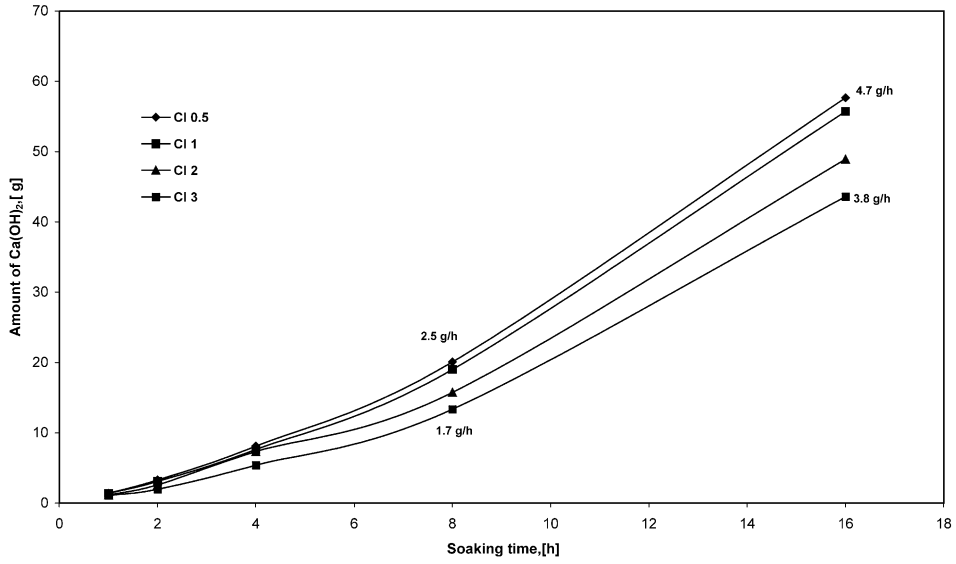

Fig. 5. Rate of hydration of the dense lime–ilmenite grains.

with relatively higher amounts in CI_3 as revealed from its point analyses Nos. 1 as well as (1 and 4) in CI_2 and CI_3, respectively. Also, some calcium silicate phases are detected in the interstitial spaces of lime particles (Nos. 3 and 4 in CI_2 and No. 3 in CI_3). Point analyses of the silicate phase seems to belong to C_3S with small amounts of R_2O_3 in solid solution.

The results of microchemistry of the coexisting phases confirm their solid phase composition as calculated in Table 2 and qualitatively determined by XRD in Fig. 3. However, the calculated calcium–alumino–ferrite (C_4AF and C_3A) as well as titanate (C_3T_2) phases are found as a solid solution of plateley calcium alumino-ferrite-titanate phase as revealed from Fig. 7 and Table 3. This is attributed to the dissolution of such low- melting calcium alumino–ferrite–titanate in the liquid phase developed on firing lime grains up to 1550°C. On cooling, the plateley Ca–alumino–ferrite titanate solid solution phase is easily solidified from such lime-rich liquid phase in the matrix of the direct- bonded lime network.

Table 3
Point analysis of lime–ilmenite dense samples

Oxide (wt.%)	CI_2				CI_3			
	(1)	(2)	(3)	(4)	(1)	(2)	(3)	(4)
SiO_2	3.10	0.75	22.71	24.95	4.47	–	10.10	1.10
Al_2O_3	8.03	–	4.36	4.53	14.16	–	–	1.57
TiO_2	14.60	–	2.59	3.17	7.00	–	–	9.76
Fe_2O_3	17.33	–	2.37	2.48	23.68	–	–	18.97
CaO	56.95	99.25	67.96	64.87	50.69	100	89.90	68.59

The results of cold crushing strength (CCS), refractoriness under load (RUL) and thermal shock resistance (TSR) of the dense and hydration-resistant lime grains are summarized in Table 4. Both of the dense CI_2 and

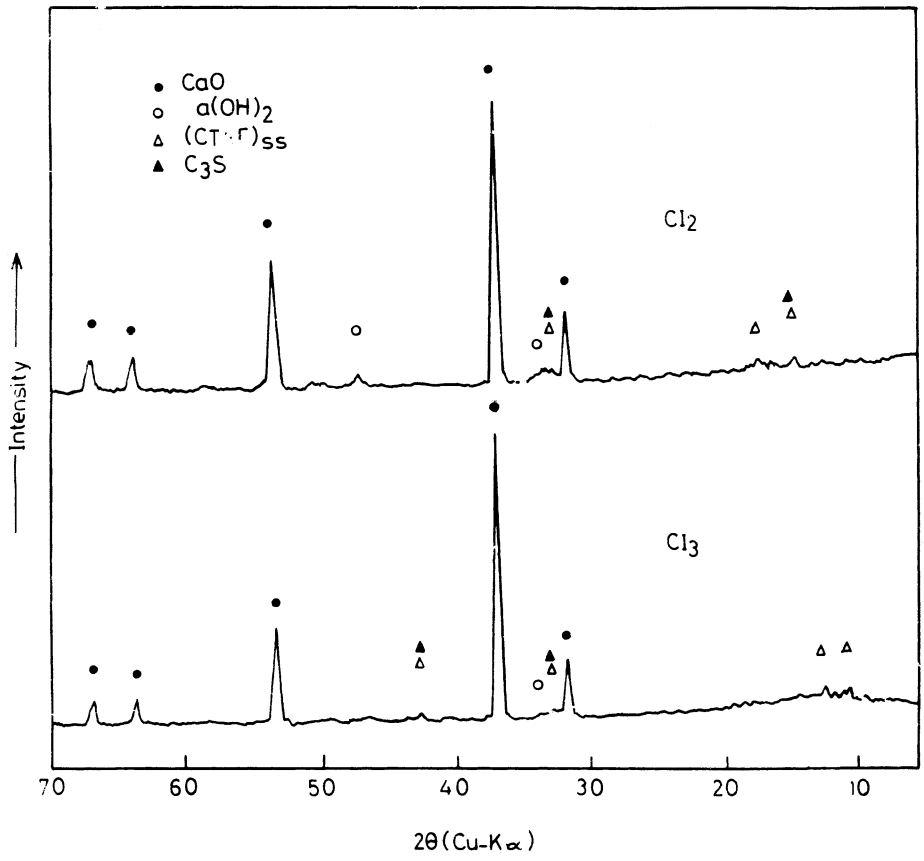

Fig. 6. XRD patterns of the dense CI_2 and CI_3 lime grains.

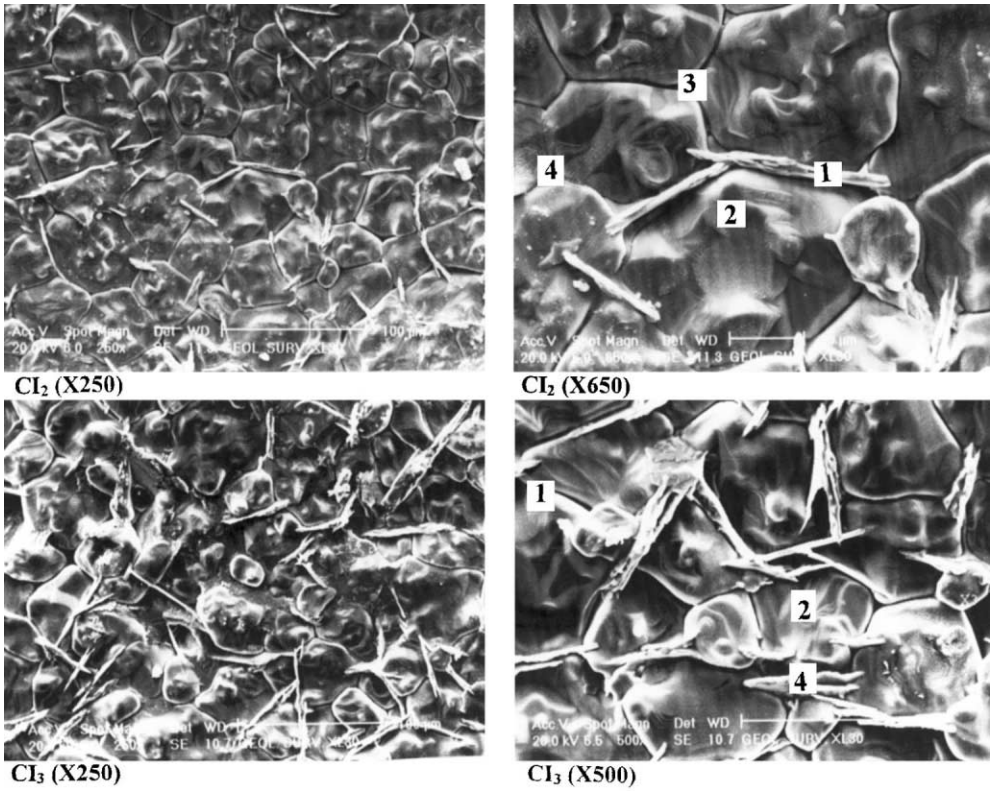

Fig. 7. SEM photomicrographs of the dense CI_2 and CI_3 lime grains.

Table 4
Technological properties of the dense selected batches

Lime grains	CCS (N/mm^2)	RUL T_a (°C)	TSR (no. of cycles)	Rate of hydration (g/h)	
				up to 8 h	up to 16 h
CI_2	89	>1500	>20	2.00	4.10
CI_3	92	>1500	>20	1.70	3.80

CI_3 lime grains shows high CCS, load- bearing capacity and resistance to thermal shock. This is mainly attributed to the compact microstructure of the direct bonded lime network with partial bonding of calcium alumino–ferrite–titanate platelets. This leads to maximize their cold crushing strength to (89–92 N/mm^2) without significant deterioration of their thermo-mechanical properties; namely temperature corresponding to beginning of subsidence under a load of 2 kg/cm^2 ($T_a > 1500°C$) and their resistance to successive cycles of sudden heating at 1000°C and cooling in air (>20 cycle). The improvement of thermo-mechanical properties is also accompanied with significant raising of the hydration resistance; the main problem for handling and storing lime refractories.

4. Conclusions

1. Economical deposits of pure limestone and ferri-ilmenite are available in Egypt at Beni Khaled, El Menya and Abu Ghalaga, Eastern Desert, respectively.
2. Dense and hydration-resistant lime grains can be processed by doping the limestone powder with 2–3 wt.% of ferri-ilmenite and firing for 2 h at 1550°C using a two-stage firing process.
3. The processed grains have also high load-bearing capacity and thermal shock resistance. Therefore, their use is recommended to substitute magnesia refractories in some primary and secondary steel-making processes.

References

[1] M.A. Serry, S.M. Naga, Characterization of precipitated magnesium and aluminum hydroxides for refractories industry, Silic. Ind. 52 (3/4) (1987) 41–46.
[2] M.A. Serry, M.F.M. Zawrah, Precipitation of pure magnesium hydroxide and calcium carbonate by treatment of calcined dolomite with recycled sucrose solution, Egyptian Patent, No. 479/97, 1997.
[3] E.A. El-Rafei, S.M. Naga, Factors influencing precipitation of pure magnesium hydroxides from sea-water and brines, Keram. Zeitschrift 31 (1979) 283.
[4] M.A. Serry, A. Barbulescu, Thermal equilibrium of MgO-dolomite refractories within the system: CaO–MgO–C_2S–C_4AF, Trans. and J. Br. Ceram. Soc. 80 (6) (1981) 196–201.
[5] M.A. Serry, M.S. Attia, Thermal equilibrium and properties of some MgO-dolomite refractories, Trans. and J. Br. Ceram. Soc. 84 (4) (1985) 142–145.
[6] M.A. Serry, M.B. El-Kholi, M.A. Mandour, Texture and properties of zircon-bearing refractory lime, Trans. and J. Br. Ceram. Soc. 85 (10) (1986) 172–174.
[7] M.I. Sayed Ahmed, A. El-Shahat, O.A. Kamel, A.A. Abdel Wahab, Petrography of some middle eocene limestones along the Nile Valley (Menia Formation), Egypt, Egypt J. Geol. 26 (2) (1982) 161–170.
[8] A.A. Hussein, M.A. El-Sharkawi, Mineral deposits, in: R. Said (Ed.), The Geology of Egypt, A.A. Balkema, Rotterdam, The Netherlands, 1990 (Chapter 26).
[9] G. Routschka (Ed.), Refractory Materials: Pocket Manual. Vulkan-Verlag, Essen, Germany, 1997.
[10] F. Nadachowski, Lime refractories, Interceram 1 (1975) 42–45.
[11] B. Brenzy, Equilibrium partial pressure of MgO, SiO_2, CaO and CoO in carbon containing doloma refractories, J. Am. Ceram. Soc. 59 (11–12) (1976) 529–530.
[12] D.H. Hubble, K.K. Kappmeyer, Slag erosion resistance of various types of BOP bricks, Am. Ceram. Soc. Bull. 45 (7) (1966) 646–669.
[13] D.H. Hubble, Some properties of lime refractories, J. Am. Ceram. Soc Bull. 48 (1969) 618.
[14] Carr, L.F. Rooney, Limestone and dolomite, American Institute of Mining, Metallurgical and Petroleum Engineers, New York, 1975, pp. 757–789.
[15] G.V. Samsonov, The Oxides Handbook, 2nd Edition, Plenum Press, New York, 1982.
[16] J.H., Chesters, Refractories production and properties, Iron and Steel Institute, London, 1973.
[17] S. Ying-Yi, G.L. Messing, L.P. Caywood, Increasing the hydration resistance of calcia, J. Am. Ceram. Bull. 67 (1984) C109.
[18] I.B. Cutler, R.L. Felix, R.C. Bradt, Reactive — phase cal-sintering of calcium carbonate derived lime, J. Am. Ceram. Soc. 67 (5) (1984) C109.
[19] F. Nadachowishi, Refractories based on lime, Ceramurgia Int. 2 (1976) 55–61.
[20] X. Liu, Y. Zhou, B. Shang, Effect of oxides on the sintering process and the hydration resistance of CaO clinkers, Interceram 45 (2) (1996).
[21] K.K. Kappmeyer, D.H. Hubble, Pitch-bearing MgO–CaO refractories in the BOP process, 1-7, in: A.M. Alper (Ed.), High-Temperature Oxides, Part 1, Academic Press, New York, 1970, pp. 1–76.
[22] M.A. Serry, N.M. Ghoneim, E.M. Hammad, Densification of lime within the CaO–ZrO_2–SiO_2 system, Silic. Ind. 52 (1987) 163.
[23] N.M. Ghoneim, M.A. Mandour, M.A. Serry, Sintering of lime doped with La_2O_3 and CeO_2, Ceram. Int. 15 (1989) 357–362.
[24] N.M. Ghoneim, M.A. Mandour, M.A. Serry, Phase composition, microstructure and properties of sintered La_2O_3-doped lime and dolomite grains, Ceram. Int. 16 (1990) 215–223.
[25] M.A. Serry, L.G. Girgis, M.A. Mandour, A.G.M. Othman, Low-flux hydration resistant dolomite grains from Egyptian raw materials, Interceram 41 (1) (1993) 20–23.
[26] M.A. Serry, M.A. Mandour, A.G.M. Othman, L.G. Girgis, Effect of some dopant materials on the microstructure of dolomitic magnesite grains, Interceram 45 (3) (1996) 162–166.
[27] E.Z. Basta, M.A. Takla, Petrological studies on Abu Ghalaga ilmenite occurrence, Eastern Desert, J. Geol. U. A. R 12 (2) (1968) 87–1243.
[28] G. Naim, Abu Ghalaga titanium, iron and vanadium ore reserves, The Arab Mining and Petrolium Trans. 39 (1983) 2–16.
[29] White, J. in: A.M. Alper (Ed.), High temperature oxides, vol. 1, Academic Press, New York, 1970, p. 77.